Macromolecules

ARTICLE

pubs.acs.org/Macromolecules

Synthesis and Characterization of Cyclic Brush-Like Polymers by *N*-Heterocyclic Carbene-Mediated Zwitterionic Polymerization of *N*-Propargyl *N*-Carboxyanhydride and the Grafting-to Approach

Samuel H. Lahasky, Wilson K. Serem, Li Guo, Jayne C. Garno, and Donghui Zhang*

Department of Chemistry and Macromolecular Studies Group, Louisiana State University, Baton Rouge, Louisiana, 70803

Supporting Information

ABSTRACT: Cyclic brush-like polymers were synthesized by tandem organo-mediated zwitterionic polymerization and a grafting-to approach. The cyclic polymer backbone, consisting of poly(*N*-propargylglycine) (*c*-PNPG), was synthesized by an *N*-heterocyclic carbene (NHC)-mediated zwitterionic ring-opening polymerization of *N*-propargyl *N*-carboxyanhydride. The polymerization proceeds in a quasi-living manner, allowing access to *c*-PNPG of well-defined chain length. The cyclic architecture of the polymers was verified by size exclusion chromatography (SEC) and mass spectroscopy (MS), as well as scanning probe characterization. Poly(ethylene glycol) functionalized with azido end-groups was subsequently grafted onto the *c*-PNPG by the copper-mediated azide/alkyne cycloaddition reaction (CuAAC). The side chain grafting density was determined by ^{1}H NMR spectroscopy and SEC analysis. The grafting efficiency is low (<19%) when the cyclic backbone is comprised of a *c*-PNPG homopolymer. The efficiency can be significantly improved (up to 93%) by utilizing cyclic poly(*N*-propargylglycine)-*ran*-poly(*N*-butylglycine) random copolymers (*c*-PNPG-*r*-PNBG). This has been attributed to the ease of access to the propargyl groups in *c*-PNPG and *c*-PNPG-*ran*-PNBG: the strong tendency of the former to aggregate in common organic solvents (including the CuAAC reaction medium) restricts access to the propargyl groups.

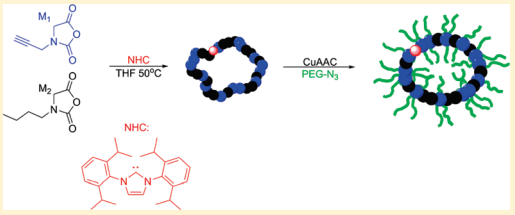

INTRODUCTION

Brush-like polymers, which consist of a backbone and a bristle, represent an interesting polymeric architecture.[1] Attachment or growth of the bristles increases the conformational strain of the backbone[2] and accordingly increases the Kuhn length and reduces the chain entanglement.[3,4] As a result, brush-like polymers have been investigated as precursors of shape-persistent organic nanotubes,[5] lubricants,[6] or self-assembled one-dimensional photonic crystals.[7,8] Brush-like polymers can be synthesized by several synthetic strategies[8] including the grafting-through,[9] the grafting-from,[10] and the grafting-to approaches.[11] The grafting-to approach is particularly versatile regarding the chemistry of brush-like polymers. As the backbone and side chains are independently prepared prior to coupling, their composition can be precisely characterized. The drawback of this method is that the grafting density is often limited by the steric congestion of the polymeric side chains.

The grafting efficiency is also significantly impacted by the method used to couple the side chains to the polymer backbone.[12] In this regard, click chemistry, particularly the copper-mediated alkyne/azide cycloaddition reaction (CuAAC),[13] has become increasingly employed in the synthesis of brush-like polymers[14] due to its high efficiency and stoichiometric bond formation under mild conditions.[11,15]

Most synthetic brush-like polymers feature a linear polymer backbone. Molecular architectures such as cyclic or star-shapes have received less attention.[16] Schappacher et al. reported the synthesis of cyclic polymer brushes bearing randomly grafted polystyrene (PS) and polyisoprene (PI) side chains. The cyclic polymer backbone was prepared by end-to-end coupling of an $\alpha-\omega$ heterofunctional linear precursor, and the PS/PI side chains were statistically grafted to the backbone in one step.[17] While the majority of the polymer brushes are cyclic, linear, tadpole or ∞-shape backbones have been evidenced by atomic force microscopy (AFM).[17,18] These architectural contaminants arise from the limitations of synthetic methods used to prepare the cyclic polymer backbone. Cyclic brush-like polymers can be synthesized by a grafting-from approach, where PS brushes are grown from a cyclic poly(ethylene glycol) backbone via nitroxide-mediated radical polymerization (NMP), as shown by Jia et al.[19] Coulembier et al. reported the synthesis of jellyfish macromolecular architectures by a grafting-through approach where a macromonomer (i.e., poly(methyl methacrylate)-modified L-lactide) was copolymerized with L-lactide in the presence of *in situ* generated *N*-heterocyclic carbene.[20] More recently, Xia et al. and Zhang et al. have synthesized macrocyclic brushes by ring expansion metathesis polymerization of functionalized norbornenes.[21] In the former report the side chains were installed prior to polymerization as part of the macromonomers, whereas in the latter case the side chains were attached by

Received: August 25, 2011
Revised: October 13, 2011
Published: November 07, 2011

CuAAC post polymerization. While the cyclic polymer backbone itself has random coil conformations, the grafting of polymeric side chains rigidifies the backbone, resulting in shape-persistent ring-like nanostructures. Many of these polymers exhibit intriguing solution and self-assembly behaviors and have potential uses in nanotechnology and biomedical sciences. Before these applications can be realized, it is important to develop robust and efficient synthetic routes toward these materials. Special attention needs to be paid to the main challenge in cyclic brush-like polymer synthesis: the construction of the cyclic backbone architecture.[22]

Cyclic polymers are typically synthesized by (1) the end-to-end coupling of a linear precursor, (2) ring−chain equilibrium, or (3) ring-expansion polymerization. In the first method, two chain ends are either homo- or heterofunctionalized to enable intramolecular coupling under conditions of high dilution. While this approach is versatile as it allows a variety of linear polymeric precursors to be synthesized by controlled polymerizations (e.g., ATRP, RAFT), additional chain-end derivation is often required to install the desired functionalities for coupling reactions. This limitation, in addition to the need for highly dilute conditions, makes this approach impractical for large scale synthesis. Recent developments in using highly efficient coupling chemistry (i.e., CuAAC or thiol−ene chemistry) under dynamic dilution conditions has dramatically improved the synthetic ease and efficiency.[23,24] Preassociation of linear chain-ends by electrostatic interaction or micelle formation have also reduced the need for high dilution.[25] However, cyclic polymers prepared by this method are typically limited to low to moderate molecular weight. Cyclization of high molecular weight linear precursors often yields topological contaminants such as knots or catenates.

The second method, ring−chain equilibrium, involves a competition between the propagation of a linear polymer and chain cyclization through backbiting of the chain ends into the growing chain. The ring−chain equilibrium cyclization is usually limited to ring-opening polymerization and thermodynamically controlled step-growth polymerization.[26] While the total percentage of cyclic species can be increased by high dilution, smaller rings are still thermodynamically favored.[27] Kricheldorf and Schwarz demonstrated that, in kinetically controlled step-growth polymerizations, cyclic polymers are the stable end-products.[28] However, the polymers tend to exhibit bimodal mass distribution where small rings are inevitably present.

Recent developments in the third method, ring-expansion polymerization (REP), have enabled the conversion of small cyclic substrates into cyclic polymers having moderate to high molecular weight.[29] The cyclic polymers obtained are of high architectural purity and their synthesis does not require high dilution conditions. For example, Bielawski et al. have reported the REP of cyclooctene using a cycloalkylidenyl-ruthenium catalyst/initatior to generate the cyclic poly(octane), which upon hydrogenation yields high MW cyclic polyethylene ($M_n \sim$ several million dalton).[29a] Li et al. have demonstrated the synthesis of cyclic polycaprolactone by REP of γ-caprolactone with a cyclic stannane catalyst/initiator.[29b] Herbert et al. reported a Lewis base-mediated ring-expansion polymerization of silicon-bridged [1]ferrocenophanes, resulting in high molecular weight cyclic metallopolymers.[29c] Waymouth, Hedrick and coworkers demonstrated that *N*-heterocyclic carbenes (NHC) can mediate the REP of cyclic esters to yield their respective cyclic polyesters.[29d−g] The limitations of the REP approach are that it requires a specially designed initiator/catalyst and that there are few suitable monomer structures. One strategy to overcome this challenge is to develop new monomers that are amenable to REP and contain side chains that are readily derivatized post-polymerization. Polymerization of these monomers will lead to cyclic polymers with diverse structures.

We have recently reported that an NHC mediates the zwitterionic ring-opening polymerization of *N*-substituted *N*-carboxyanhydrides to yield cyclic poly(*N*-substituted glycine) [aka poly(α-peptoids)].[29h,i] The reaction proceeds in a quasi-living manner and enables the controlled synthesis of the cyclic poly(α-peptoid) homopolymers or block copolymers. In the zwitterionic polymerizations, the *N*-substituent has been limited to inert aliphatic[29h] or aryl groups[29i] to ensure living polymerization. This significantly limits the structural diversity of the poly(α-peptoid)s. With demonstrated biocompatibility and enhanced proteolytic stability,[30,31] poly(α-peptoid)s are potentially useful for various biotechnological applications (e.g., drug delivery, and bioactive coatings). For these applications, it is important that differing functionalities can be readily installed on the side chains so as to confer the desired properties. In this work, we extend the methodology toward the polymerization of *N*-propargyl NCA to yield cyclic poly(*N*-propargyl glycine) (*c*-PNPG) and examine its copolymerization with *N*-butyl NCA to produce cyclic poly(*N*-propargyl glycine)-*ran*-poly(*N*-butyl glycine) random copolymers (*c*-PNPG-*r*-PNBG). We demonstrate that the propargyl side chain can be readily functionalized with an azido-terminated poly(ethylene glycol) by CuAAC chemistry, producing a water-soluble cyclic brush-like polymer.

EXPERIMENTAL SECTION

Materials. Glyoxylic acid monohydrate (98%), progargyl amine (98%), butyl amine (98%), di-*tert*-butyl dicarbonate (97%), triethylamine, copper(I) bromide, PMDETA, and phosphorus trichloride were purchased from Sigma-Aldrich and used as received. All solvents used in this study were purchased from Sigma-Aldrich and purified by passing through alumina columns under argon. The compounds 2,6-diisopropylphenylimidazol-2-ylidene (NHC)[32] and azido terminated poly(ethylene glycol) (PEG-N_3) (M_n = 2 kg·mol^{-1}, PDI = 1.03; M_n = 500 g·mol^{-1}, PDI = 1.05) were synthesized by reported procedures.[33] Butylamine was stirred over CaH_2 overnight and distilled under vacuum prior to use as an initiator. The compounds of *N*-propargyl NCA (M_1) and *N*-butyl NCA (M_2) were synthesized by adapting a literature procedure.[29h]

Instrumentation. The ^{1}H and ^{13}C{^{1}H} NMR spectra were recorded on a Bruker AV-400 spectrometer, and the chemical shifts were referenced in parts per million (ppm) relative to proton impurities or ^{13}C isotopes of $CDCl_3$ respectively. The FTIR spectra were collected on a Bruker Tensor 27 FTIR spectrometer. The ESI spectra were recorded on an Agilent 6710 TOF mass spectrometer in the positive ion mode. The SEC analyses were conducted using an Agilent 1200 system (Agilent 1200 series degasser, isocratic pump, auto sampler and column heater) equipped with three Phenomenex 5 μm, 300 × 7.8 mm columns [100 Å, 1000 Å and Linear(2)], Wyatt DAWN EOS multiangle light scattering (MALS) detector (GaAs 30 mW laser at λ = 690 nm), Wyatt ViscoStar viscometry (VISC) detector and Wyatt Optilab rEX differential refractive index (DRI) detector with a 690 nm light source. DMF containing 0.1 M LiBr was used as the eluent at a flow rate of 0.5 mL·min^{-1}. The column temperature was 50 °C and the detector temperature was 25 °C. All data analyses were performed using Wyatt Astra V 5.3 software. Polymer molecular weight (M_n) and molecular weight distribution (PDI) were obtained by two methods: (1) Zimm model fit of MALS-DRI data; (2) conventional SEC analysis with a calibration curve. The calibration curve was constructed from

Scheme 1

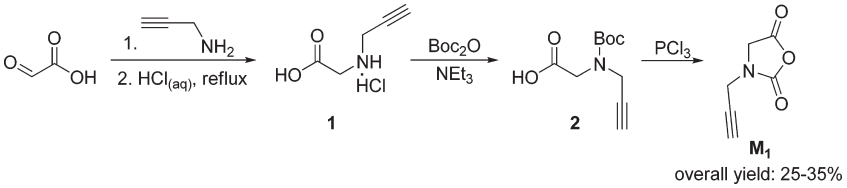

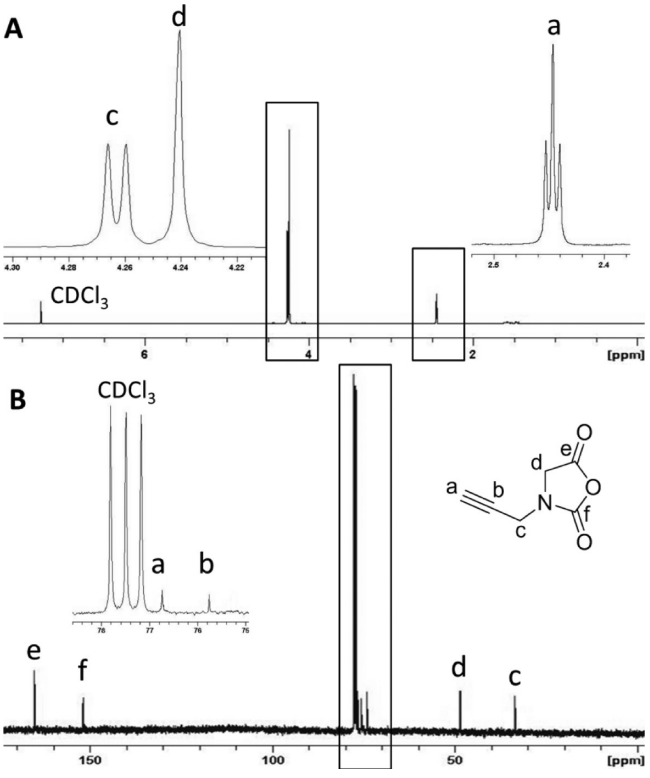

Figure 1. (A) ^{1}H NMR and (B) ^{13}C {^{1}H} NMR spectra of *N*-propargyl NCA (M_1) in $CDCl_3$.

23 pauci-disperse polystyrene standards (M_n = 590 g·mol^{-1} to 1472 kg·mol^{-1}, Polymer Laboratories, Inc.) using Astra's column calibration template. Relative M_n and PDI were then calculated using Astra's conventional calibration template. Dynamic light scattering (DLS) analysis was conducted on a Malvern Zetasizer Nano-ZS instrument while using the Zetasizer software version 6.12. The *c*-PNPG polymer solution was prepared by filtering through a 0.2 μm PTFE filter prior to DLS data collection.

Refractive Index Increment (d*n*/d*c*) Measurement. The refractive index increment (d*n*/d*c*) of the synthesized polymers was measured using Wyatt's rEX DRI detector and Astra software d*n*/d*c* template. Six polymer/DMF/0.1 M LiBr solutions with different and precise concentrations of polymer were sequentially injected into the DRI detector. The measured refractive index values were plotted versus concentration. The slope from a linear fitting of the data is the d*n*/d*c* of the polymer. The measured d*n*/d*c* values of *c*-PNPG and *l*-PNPG in LiBr (0.1 M)/DMF at 25 °C and 690 nm wavelength are 0.1094(14) mL·g^{-1} and 0.1012(7) mL·g^{-1} respectively.

Intrinsic Viscosity Measurement. Eight polydisperse cyclic or linear poly(*N*-propargylglycine) samples with different molecular weight were independently prepared from NHC or butylamine-mediated polymerizations of M_1. Polydisperse cyclic (M_n = 14.8 kg·mol^{-1}, PDI = 1.70) and linear poly(*N*-propargylglycine) samples (M_n = 9.3 kg·mol^{-1}, PDI = 1.55) were prepared by mixing the four pauci-disperse polymers with different molecular weight in equal weight fractions. The polydisperse samples were then analyzed by SEC−MALS−VISC−DRI for their intrinsic viscosities ([η]) and the absolute molecular weights.

Atomic Force Microscopy (AFM). Imaging of the cyclic brush-like polymers was accomplished using tapping mode AFM (Agilent 5500 AFM/SPM system) in ambient air with Picoscan v5.3.3 software with probes acquired from Vista probes. The driving frequency for the tip during the imaging of the polymers was 181 kHz. Polymer samples were dissolved in chloroform to make a final concentration of 0.02 mg·mL^{-1}. A volume of polymer solution (~15 μL) was drop-deposited and dried on freshly cleaved mica (0001) in ambient conditions for 24 h before AFM imaging. Minimal processing of the images was done using Picoscan software from Agilent.

Synthesis of 2-(Prop-2-yn-1-ylamino)acetic Acid Hydrochloric Salt (1). Propargyl amine (5.0 g, 90.8 mmol) and glycoxylic acid (16.72 g, 225 mmol) were both dissolved in CH_2Cl_2 (230 mL) and allowed to react overnight at room temperature. The CH_2Cl_2 was removed under reduced pressure and aqueous HCl (137 mL, 137 mmol, 1.0 M) was added. The solution was heated at reflux for 24 h, after which the water was removed by rotary evaporation. The resulting solid was redissolved in methanol and precipitated by the addition of copious volumes of ether. The product was collected by filtration and dried under vacuum to yield a brown solid (8.55 g, 63% yield). ^{1}H NMR (400 MHz, D_2O), δ: 10.03 (s, −O*H*, 1H), 4.04 (d, −CH_2, 2H), 3.87 (t, −CH_2CH, 2H), 2.35 (t, −C*H*, 1H). ^{13}C {^{1}H} NMR (100 MHz, D_2O) δ: 173.8 (−CO−), 82.9 (−C≡), 73.3 (≡CH), 50.4 (NHCH_2CO), 40.1 (≡CCH_2NH−).

Synthesis of 2-((*tert*-Butoxycarbonyl)(prop-2-yn-1-yl)-amino)acetic Acid (2). The compound **1** (6.0 g, 40.1 mmol) was dissolved in distilled water (135 mL), to which di-*tert*-butyl dicarbonate (29.3 g, 134 mmol) and triethylamine (37.4 mL, 268 mmol) were sequentially added. The reaction mixture was stirred overnight at room temperature and then washed with hexane to remove any unreacted di-*tert*-butyl dicarbonate. The aqueous phase was separated and made acidic (pH = 3) with 1 N HCl(aq). The product was extracted into ethyl acetate (3 × 100 mL) and the organic layer was combined and washed with a saturated aqueous NaCl solution, dried over anhydrous $MgSO_4$, and concentrated to afford a beige solid. ^{1}H NMR (400 MHz, $CDCl_3$), δ: 4.13 (t, −CH_2−, 2H), 4.07 (s, −CH_2−, 2H), 2.33 (t, −C*H*, 1H), 1.46 (d, −(CH_3)$_3$, 9H). ^{13}C {^{1}H} NMR (100 MHz, $CDCl_3$) δ: 173.4 (−COOH), 154.8 (−NCOO−), 80.5 (−OC(CH$_3$)$_3$), 78.9 (≡C−), 73.0 (≡CH), 54.5 (−NCH_2COOH), 40.1 (≡CCH_2N−), 28.0 (−(CH_3)$_3$).

Synthesis of *N*-Propargyl *N*-Carboxyanhydride (M_1). The compound **2** (1.74 g, 6.5 mmol) was dissolved in anhydrous CH_2Cl_2 (230 mL) under a nitrogen atmosphere. PCl_3 (1.15 mL, 13.1 mmol) was added dropwise to the solution at 0 °C. The reaction mixture was stirred for 3 h and the solvent was removed under vacuum. The solid residue was extracted with anhydrous CH_2Cl_2 (20 mL) and filtered. The filtrate was evaporated to afford a white solid. Further purification by recrystallization from anhydrous CH_2Cl_2/hexane and sublimation yielded white crystals (0.5 g, 55% yield). ^{1}H NMR (400 MHz, $CDCl_3$) δ: 4.27

dx.doi.org/10.1021/ma201948u |*Macromolecules* 2011, 44, 9063–9074

Scheme 2

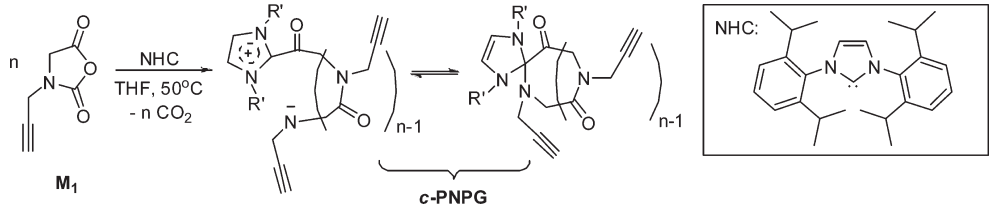

Table 1. NHC-Mediated Polymerization of M_1 and Copolymerization of M_1 and M_2

entry	polymer	$[M_1]_0$:$[M_2]_0$:$[NHC]_0$[a]	M_n(theor.)[b] (kg·mol^{-1})	M_n(SEC)[c,d] (kg·mol^{-1})	M_n(NMR) (kg·mol^{-1})	PDI	convn[e]
1	*c*-PNPG	25:0:1	2.4	-	2.2	-	100
2	*c*-PNPG	50:0:1	3.8	4.3[c]	4.1	1.10[c]	100
3	*c*-PNPG	75:0:1	5.5	5.7[c]	5.8	1.03[c]	100
4	*c*-PNPG	100:0:1	9.1	9.1[c]	10.9	1.13[c]	96
5	*c*-PNPG	122:0:1	11.6	13.3[c]	11.5	1.12[c]	100
6	*c*-PNPG	200:0:1	18.1	15.6[c]	-	1.10[c]	95
7	*c*-PNPG$_{159}$-*r*-PNBG$_{173}$	150:150:1	20.5	44.6[d]	43.2	1.12[d]	99
8	*c*-PNPG$_{150}$-*r*-PNBG$_{30}$	250:50:1	29.4	49.2[d]	17.7	1.15[d]	99
9	*c*-PNPG$_{102}$-*r*-PNBG$_{73}$	100:133:1	24.1	49.9[d]	17.7	1.30[d]	90
10	*c*-PNPG$_{103}$-*r*-PNBG$_{35}$	76:24:1	9.9	56.0[d]	13.7	1.20[d]	99
11	*c*-PNPG$_{62}$-*r*-PNBG$_{49}$	50:50:1	10.5	38.9[d]	10.9	1.14[d]	99
12	*c*-PNPG$_{39}$-*r*-PNBG$_{99}$	20:80:1	11.1	37.1[d]	14.9	1.11[d]	99

[a] $[M_1]_0$=$[M_2]_0$= 0.4 M for all polymerizations. [b] Theoretical molecular weights were calculated from the $[M_1]_0$:$[M_2]_0$:$[NHC]_0$ ratio and the conversion of monomer to polymer (Note: the 6MR content is subtracted in the calculation). [c] Experimental molecular weight and polydispersity index were determined by a tandem SEC−MALS−DRI system in LiBr (0.1 M)/DMF solution at 50 °C using a measured d*n*/d*c* of 0.1094(14) mL·g^{-1}. [d] Experimental molecular weight and polydispersity index were determined by a SEC−DRI system in LiBr (0.1M)/DMF solution at 50 °C using polystyrene standards. [e] Monomer conversions were determined by FTIR spectroscopy.

(d, −C*H*$_2$−, 2H), 4.24 (s, −C*H*$_2$−, 2H), 2.45 (t, ≡C*H*, 1H). ^{13}C{^{1}H} NMR (100 MHz, $CDCl_3$) δ: 165.5 (−CH$_2$*C*(O)O−), 151.4 (−O*C*(O)N−), 77.7 (*C*H≡), 76.8 (≡*C*−), 49.2 (≡CCH$_2$N−), 32.6 (C(O)*C*H$_2$N−).

Representative Synthetic Procedure for the Cyclic Poly(*N*-propargylglycine) (*c*-PNPG). Inside a glovebox, M_1 (200 mg, 1.44 mmol) was dissolved in THF (2.5 mL) to which a THF stock solution of NHC (267 μL, 14.4 μmol, 53.8 mM) was added at room temperature. The reaction was stirred and heated at 55 °C for 18 h. An excess of hexane (10 mL) was added to the remaining reaction mixture. The suspension was stirred at 50 °C for 8 h and filtered while still warm to remove low molecular weight oligomers. The yellow solid that was obtained was dried under vacuum (120 mg, 88% yield). ^{1}H NMR (400 MHz, $CDCl_3$), δ: 4.67−4.04 (bm, −COC*H*$_2$N−, −CC*H*$_2$N−, 4H), 2.66−2.30 (bm, −CC*H*, 1H). ^{13}C{^{1}H} NMR (100 MHz, $CDCl_3$) δ: 163.4 (*C*=O), 76.6 (H*C*≡), 73.9 (*C*≡), 48.8 (*C*H$_2$C=O), 35.0 (*C*H$_2$C≡).

Representative Synthetic Procedure for the Linear Poly(*N*-propargylglycine) (*l*-PNPG). Inside a glovebox, M_1 (91 mg, 0.654 mmol) was dissolved in THF (2.5 mL) to which a THF stock solution of butyl amine (143 μL, 7.69 μmol, 53.8 mM) was added at room temperature. The solution was degassed by freeze−pump−thaw cycle three times and left to react under reduced pressure in a sealed flask. The reaction was stirred and heated at 50 °C for 48 h. An excess of hexane (10 mL) was added to the remaining reaction mixture. The suspension was stirred at 50 °C for 8 h and filtered while still warm to remove low molecular weight oligomers. The white solid that was obtained was dried under vacuum (31 mg, 50% yield). ^{1}H NMR (400 MHz, $CDCl_3$), δ: 4.67−4.04 (bm, −COC*H*$_2$N−, −CC*H*$_2$N−, 4H), 2.66−2.30 ^{13}C{^{1}H} NMR (100 MHz, $CDCl_3$) δ: 162.1 (*C*=O), 75.9 (H*C*≡), 73.1 (*C*≡), 49.1 (*C*H$_2$C=O), 38.4 (*C*H$_2$C≡).

Representative synthetic procedure for the cyclic poly(*N*-propargylglycine)-*ran*-poly(*N*-butylglycine) random copolymers (*c*-PNPG$_n$-*r*-PNBG$_m$). In a glovebox, M_1 (64 mg, 0.46 mmol) and *N*-butyl NCA (M_2) (72 mg, 0.46 mmol) were dissolved in anhydrous THF (4 mL). A stock solution of NHC in THF (91 uL, 2.83 μmol, 31.1 mM) was added to the reaction flask. The flask was sealed and stirred at 55 °C for 2 d. The polymerization was terminated by adding cold hexane (20 mL). The precipitated polymer was isolated by decantation and dried under vacuum (52 mg, 54% yield). ^{1}H NMR (400 MHz, $CDCl_3$), δ: 4.64−3.90 (bm, −CC*H*$_2$N−, −NC*H*$_2$CO−, −NC*H*$_2$CO, 6H), 3.51−3.20 (bm, −CH$_2$C*H*$_2$N−, 2H); 2.62−2.25 (bm, −CC*H*, 1H), 1.58−1.21 (bm, −CH$_2$C*H*$_2$CH$_2$−, CH$_3$C*H*$_2$−, 4H), 1.06−0.76 (bm, C*H*$_3$CH$_2$−, 3H).

Representative Synthetic Procedure for the Cyclic PEG-Grafted Poly(*N*-propargylglycine) (*c*-PNPG-*g*-PEG). Inside a glovebox, *c*-PNPG$_{137}$ (85.5 mg, $[propargyl]_0$ = 0.87 mmol, M_n = 13.4 kg·mol^{-1}, PDI = 1.16) was dissolved in CH_2Cl_2 (3 mL) along with PEG-N$_3$ (288 mg, 0.14 mmol, M_n =2.0 kg·mol^{-1}, PDI = 1.03, $[N_3]_0$:$[propargyl]_0$ = 1:6). A measured volume of CH_2Cl_2 stock solution containing CuBr/PMDETA (1.70 mL, 0.202 mmol, 119 mM, $[CuBr]_0$:$[PMDETA]_0$:$[propargyl]_0$ = 23:23:100) was added to the solution which was then stirred at room temperature for 3 h. The copper catalyst was removed by passing through an alumina column, and the grafted copolymer was precipitated by adding an excess of hexane and dried under vacuum at 25 °C (165 mg, 44% yield, grafting density: 19%). ^{1}H NMR (400 MHz, $CDCl_3$) δ: 7.62−8.24 (bs, −NC=C*H*N−, 1.00 H), 4.75−4.12 (bm, −NC*H*$_2$CO−, CC*H*$_2$N−), 3.97−3.45 (bm, −C*H*$_2$C*H*$_2$O−), 3.43−3.26 (bs, −CH$_2$CH$_2$OC*H*$_3$), 2.26−2.23 (bs, −CC*H*, 4.21H).

dx.doi.org/10.1021/ma201948u |*Macromolecules* 2011, 44, 9063–9074

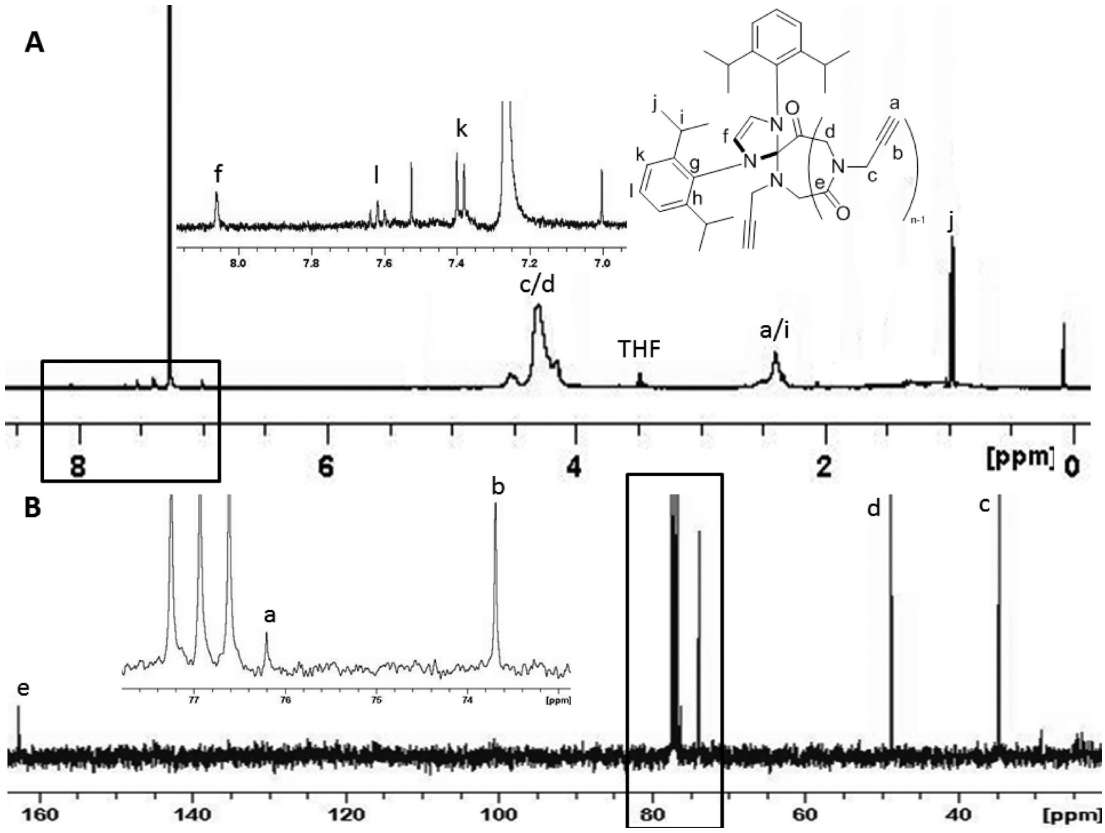

Figure 2. (A) ^{1}H NMR and (B) ^{13}C $\{^{1}$H$\}$ NMR spectra of *c*-PNPG (M_n = 4.3 kg·mol^{-1}, PDI = 1.10) in $CDCl_3$.

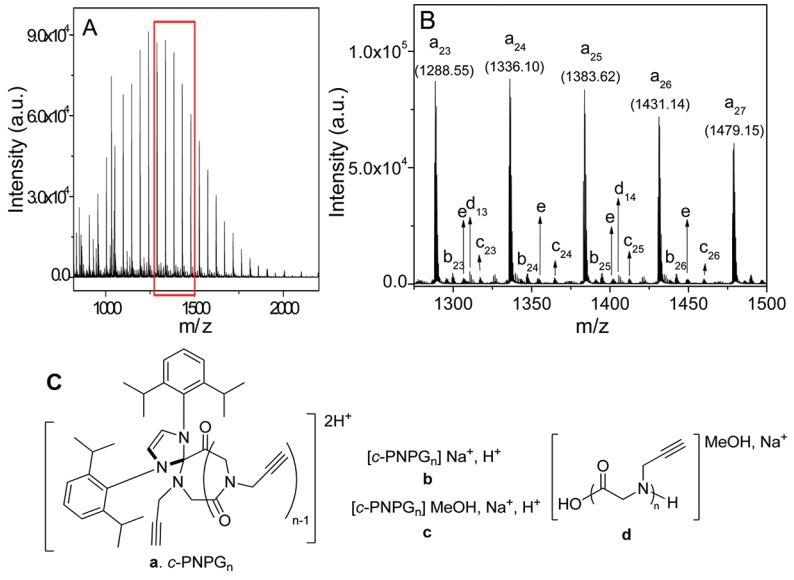

Figure 3. (A) Representative full and (B) expanded ESI MS spectra of a low molecular weight *c*-PNPG (M_n = 2.8 kg·mol^{-1}, PDI = 1.09) as well as (C) their assigned molecular structures.

Representative synthetic procedure for the cyclic PEG-grafted poly(*N*-propargylglycine)-*ran*-poly(*N*-butylglycine) random copolymers [(*c*-PNPG-*r*-PNBG)-*g*-PEG]. Inside a glovebox, *c*-$PNPG_{166}$-*r*-$PNBG_{33}$ (72.8 mg, $[propargyl]_0$ = 0.62 mmol) and PEG-N_3 (465 mg, 0.85 mmol, M_n = 550 g·mol^{-1}, PDI = 1.05, $[N_3]_0$:$[propargyl]_0$ = 1.4:1) were both dissolved in CH_2Cl_2 (5 mL). A measured volume of CH_2Cl_2 stock solution containing CuBr/PMDETA (1.70 mL, 0.202 mmol, 119 mM, $[Cu]_0$:$[PMDETA]_0$:$[propargyl]_0$ = 33:33:100) was added to the solution which was then stirred at 40 °C for 3 h. The reaction mixture was then passed through a silica column. The filtrate was concentrated and cold hexane was added to precipitate the polymer (172 mg, 42% yield, grafting density: 42%). ^{1}H NMR (400 MHz, $CDCl_3$) δ:

dx.doi.org/10.1021/ma201948u |*Macromolecules* 2011, 44, 9063–9074

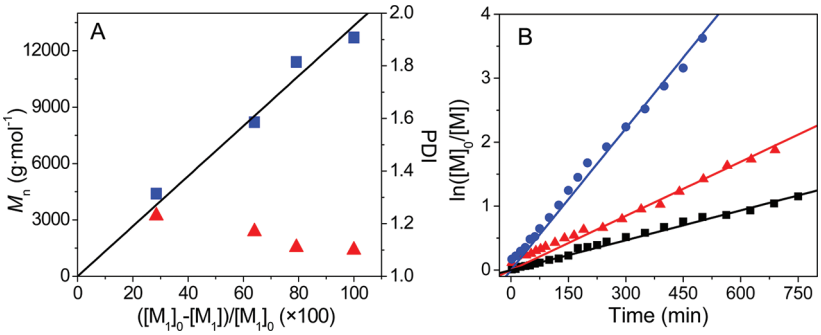

Figure 4. (A) Plot of M_n (■) and PDI (▲) versus conversion (i.e., $([M_1]_0-[M_1])/[M_1]_0$) for NHC-mediated polymerization of M_1 (THF, 50 °C) and the linearly fitted curve for the M_n-vs-conversion data (−). (Note: the monomer conversion was determined by FTIR spectroscopy while M_n and PDI were measured by SEC-MALS-DRI in LiBr (0.1 M)/DMF solution [dn/dc = 0.1094(14) mL·g^{-1}]); (B) plot of $\ln([M_1]_0/[M_1])$ versus time for the NHC-mediated polymerization of M_1 and their linearly fitted curves ($[NHC]_0$ = 3.0 (■), 4.4(▲), 12.2 mM (●); $[M_1]_0$:$[NHC]_0$ = 50:1; THF; 50 °C).

7.62−8.24 (bs, −NC=C*H*N−, 1.00 H), 4.87−4.18 (bm, −NCH_2CO−, CCH_2N−, −NCH_2CO−), 4.04−3.47 (bm, −CH$_2$CH_2O−, −CH$_2$CH$_2$N−), 3.43−3.26 (bs, −CH$_2$CH$_2$OCH_3), 2.26−2.23 (bs, −CC*H*), 1.58−1.21 (bm, −CH$_2$CH_2CH$_2$−, CH$_3$CH_2−), 1.06−0.76 (bm, CH_3CH$_2$−, 2.93 H). CH$_2$CH$_2$OCH_3), 2.26−2.23 (bs, −CC*H*), 1.58−1.21 (bm, −CH$_2$CH_2CH$_2$−, CH$_3$CH_2−), 1.06−0.76 (bm, CH_3CH$_2$−, 2.93 H).

Representative synthetic procedure for linear PEG-grafted poly(*N*-propargylglycine)-*ran*-poly(*N*-butylglycine) random copolymers [(*l*-PNPG-*ran*-PNBG)-*g*-PEG]. Inside a glovebox, *l*-PNPG$_{250}$-*r*-PNBG$_{50}$ (17.0 mg, $[propargyl]_0$= 0.14 mmol) and PEG-N$_3$ (201 mg, 0.37 mmol, M_n = 550 g·mol^{-1}, PDI = 1.05, $[N_3]_0$:$[propargyl]_0$ = 2.6:1) were both dissolved in CH_2Cl_2 (1 mL). A measured volume of CH_2Cl_2 stock solution containing CuBr/PMDETA (388 μL, 46 μmol, 119 mM, $[Cu]_0$:$[PMDETA]_0$:$[propargyl]_0$ = 33:33:100) was added to the solution which was stirred at 40 °C for 3 h. The reaction mixture was passed through a silica column. The collected filtrate was concentrated and cold hexane was added to precipitate the polymer (54 mg, 57% yield, grafting density: 63%). ^{1}H NMR (400 MHz, $CDCl_3$) δ: 7.62−8.24 (bs, −NC=C*H*N−, 1.00H), 4.87−4.18 (bm, −NCH_2CO−, CCH_2N−, −NCH_2CO−), 4.04−3.47 (bm, −CH_2CH_2O−, −CH$_2$CH_2N−), 3.43−3.26 (bs, −CH$_2$CH$_2$OCH_3), 2.26−2.23 (bs, −CC*H*), 1.58−1.21 (bm, −CH$_2$CH_2CH$_2$−, CH$_3$CH_2−), 1.06−0.76 (bm, CH_3CH$_2$−, 0.97 H).

■ RESULTS AND DISCUSSION

Synthesis and Characterization of Cyclic and Linear Poly(*N*-propargylglycine) (*c*/*l*-PNPG). The monomer *N*-propargyl NCA (M_1) was successfully synthesized on a multigram scale by the Fuch method, i.e., PCl_3-mediated cyclization of the corresponding *N*-Boc-*N*-propargylglycine precursor **2** (Scheme 1). The molecular structure of M_1 was unambiguously verified by ^{1}H and ^{13}C {^{1}H} NMR spectroscopy (Figure 1). The monomer is a white solid at room temperature and can be readily purified by sublimation prior to polymerization.

Polymerization of M_1 was achieved by heating different initial monomer to initiator ratios ($[M_1]_0$:$[NHC]_0$) in THF solution at 50 °C for 18 h under a nitrogen atmosphere (Scheme 2). Aliquots of the reaction mixtures were spectroscopically analyzed to monitor conversion of M_1 to the polymer. Both ^{1}H NMR or FTIR spectroscopy, where M_1 exhibits two characteristic $\nu_{C=O}$ stretching modes at 1859 and 1786 cm^{-1} (Figure S1, Supporting Information) were used to monitor the conversion. All reactions reached high or quantitative monomer conversion (95−100%) under these conditions (Table 1). In addition to polymer formation, ^{1}H NMR and ESI MS analysis of the reaction mixture also reveals the formation of 1,4-di(prop-2-ynyl)piperazine-2,5-dione (6MR) along with cyclic and linear oligomers in small quantities, presumably formed by an intramolecular "backbiting" mechanism (Figures S2 and S3, Supporting Information).[29i] The 6MR constitutes less than 15% of the reaction product (Figure S4, Supporting Information). Heating of the isolated and purified polymers can cause further depolymerization to yield 6MR. This is in contrast to our previous study on NHC-mediated polymerization of *N*-alkyl NCA (alkyl: Me, Bu) where no "backbiting" products were observed.[29h] The polymer products were precipitated by the addition of excess room temperature hexane. Further purification was achieved by extraction into warm hexane (50 °C), which removes cyclic oligomers. The samples were dried under vacuum prior to further analysis.

The ^{1}H NMR analysis of a low molecular weight polymer reveals three broad resonances in the ^{1}H NMR spectrum (parts a, c, and d of Figure 2A), consistent with the targeted poly(*N*-propargyl glycine) backbone structure (*c*-PNPG) (Scheme 2). In addition, resonances due to NHC moieties are also evident in the ^{1}H NMR spectrum, in agreement with NHC initiator being affixed to the polymer chain ends as previously reported (Scheme 2).[29h,i] The ^{13}C{^{1}H} NMR spectrum (Figure 2B) is also consistent with the PNPG backbone structure. The ESI MS analysis of a low molecular weight polymer reveals a major set of doubly charged mass ions whose mass equals to the sum of integer number of the desired repeating unit mass (95.10), one NHC mass (388.29) and two proton masses (1.01), in agreement with a cyclic PNPG polymeric species with one NHC moiety attached (part a, Figure 3A−C). Apart from the major species, several minor sets of mass ions that are consistent with PNPG polymeric species with different end groups or co-ionized with solvent molecules are also present. For example, doubly charged mass ions indicated by *b* and *c* are due to the *c*-PNPGs with NHC attached that are co-ionized by Na^+ and a proton (*b*) or Na^+, a proton and a solvent molecule (*c*). The mass ions indicated by *d* are the singly charged linear PNPG bearing carboxyl and amino chain ends, presumably formed by the reaction between *c*-PNPG having NHC attached with adventitious moisture.[34] The end groups for the PNPG polymeric mass ions indicated by *e* have yet to be determined. The MALDI−TOF MS analysis of the low molecular weight polymer sample also corroborates the ESI MS results (Figure S5, Supporting Information). In the MALDI−TOF MS experiment, it is critical to use a soft matrix such as α-cyano-4-hydroxycinnamic acid (CHCA) so that the original polymers remain structurally intact upon desorption and ionization.

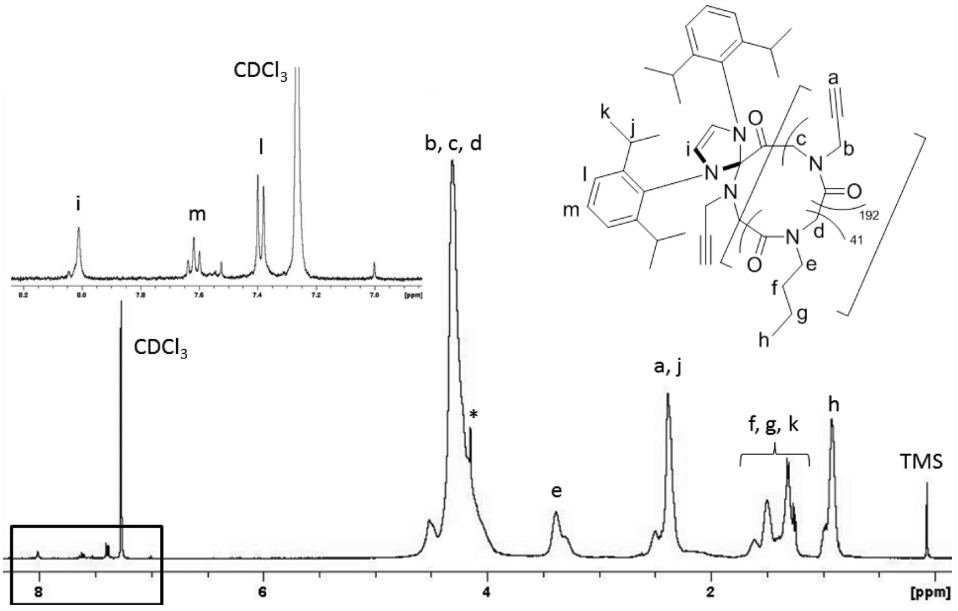

Figure 5. Representative ^{1}H NMR spectra of *c*-PNPG$_{192}$-*r*-PNBG$_{41}$ random copolymer in $CDCl_3$. (* indicates peak due to the residual M_1 monomer).

Scheme 3. R′= 2,6-Diisopropylphenyl)

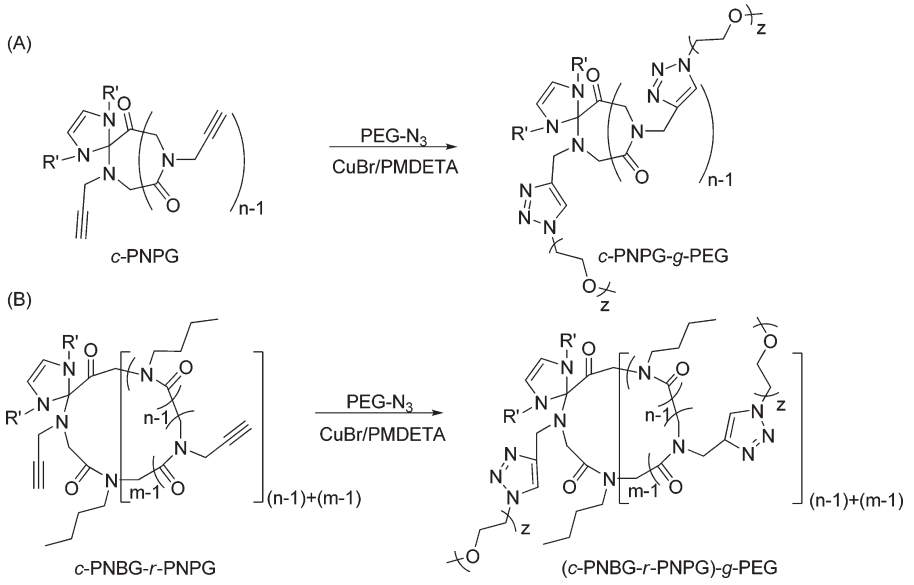

We have previously shown that the NHC moieties that are attached to the polymers are photolabile.[34] Strong laser power or a hard matrix such as dithranol causes the NHC to dissociate from the polymers.

The polymers were analyzed by ^{1}H NMR and SEC-MALS-DRI techniques for their molecular weight and molecular weight distribution. The polymer molecular weights (M_n) were determined by integrating the *c*-PNPG methine proton (a, Figure 2A) and the NHC phenyl protons (k, Figure 2A) to give the number-average degree of polymerization (DP_n), assuming that each polymer chain has one NHC affixed to it. Polymerization of M_1 with increasing $[M_1]_0$:$[NHC]_0$ leads to the formation of *c*-PNPG with increasing polymer molecular weight (M_n = 2.2−15.6 kg·mol^{-1}) and relative narrow molecular weight distribution (PDI = 1.03−1.13) (entry 1−6, Table 1). The experimental molecular weight agrees reasonably well with the theoretical values based on single-site initiation and living polymerization. Furthermore, NHC-mediated polymerization of M_1 also exhibits a linear increase of molecular weight over conversion while the molecular weight distribution remains narrow (PDI = 1.10−1.23) (Figure 4A), suggesting a constant concentration of propagating species throughout the reaction course, indicative of a living polymerization. Kinetic studies reveal that the polymerization is first-order dependent on the monomer and NHC concentration [i.e., $d[M_1]/dt=k_p[NHC]_0[M_1]$, k_p= 32 (2) $M^{-1}\cdot h^{-1}$] (Figure 4B and S6). The plots of $\ln([M_1]_0/[M_1])$ versus time (Figure 4B) all pass through (0,0), consistent with an initiation that is fast or comparable to the propagation.[35]

dx.doi.org/10.1021/ma201948u |*Macromolecules* 2011, 44, 9063–9074

The SEC chromatograms of *c*-PNPGs exhibit a multimodal distribution (Figure S7, Supporting Information) in common organic solvents [e.g., THF, $CHCl_3$ and LiBr (0.1M)/DMF] regardless of the molecular weight range. This is in contrast to MS results where only a monomodal distribution of mass ions was observed (Figure 3A and S5). The DLS analysis of *c*-PNPG reveals the presence of large particles having nonuniform size. The size of the particles increases from ~10 nm to several micrometer over 3 h in THF, strongly suggesting polymer aggregation (Figure S8, Supporting Information). Aggregation in solution appears to be an innate property of the PNPG polymer rather than being induced by the zwitterionic chain ends, since the linear poly(*N*-propargyl glycine)s (*l*-PNPG) that are independently prepared by primary amine-initiated polymerization of M_1 (Figure S9 and Table S1, Supporting Information)[29h] also exhibit multimodal SEC chromatograms in spite of their neutral chain ends (Figure S10, Supporting Information). This is in contrast to cyclic poly(*N*-butyl glycine)s (*c*-PNBG) that do not appear to substantially aggregate, as supported by monomodal SEC chromatograms.[29h] In view of this evidence, we attribute the high molecular weight components in the SEC chromatograms of PNPGs (i.e., at low elution time) to polymer aggregation. The polymer molecular weights (M_n) determined from the SEC mode at long elution times agree reasonably well with those determined by ^{1}H NMR analysis (entry 1−6, Table 1).

A comparison of SEC chromatograms of *l*-PNPG and *c*-PNPG having identical polymer molecular weight reveals that the *l*-PNPG elutes at a shorter elution time than the *c*-PNPG (Figure S10, Supporting Information), consistent with the cyclic polymers being hydrodynamically more compact than their linear analogues. Intrinsic viscosity measurement is often conducted to verify the polymer architecture.[29a,d,h,i] However, it was proven difficult for the analysis of *l*-PNPG and *c*-PNPG due to their strong tendency to aggregate in common organic solvents. As a result, the intrinsic viscosity difference observed for *l*-PNPG and *c*-PNPG of identical molecular weight cannot be unambiguously attributed to differences in their molecular architecture or their aggregation state (Figure S11, Supporting Information).

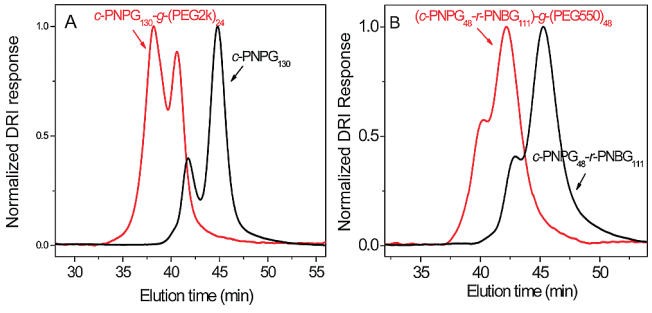

Figure 6. (A) Representative SEC chromatograms [LiBr (0.1M)/DMF, 50 °C] of *c*-$PNPG_{130}$ and *c*-$PNPG_{130}$-*g*-$(PEG2k)_{24}$ obtained after grafting of PEG by CuAAC chemistry; (B) representative SEC chromatograms [LiBr (0.1M)/DMF, 50 °C] of *c*-$PNPG_{48}$-*r*-$PNBG_{111}$ and (*c*-$PNPG_{48}$-*r*-$PNBG_{111}$)-*g*-$(PEG550)_{48}$ obtained after grafting of PEG by CuAAC chemistry.

Synthesis and Characterization of Cyclic Poly(*N*-propargyl glycine)-*ran*-poly(*N*-butyl glycine) Random Copolymers (*c*-PNPG-*r*-PNBG). Cyclic poly(*N*-propargyl glycine)-*ran*-poly(*N*-butyl glycine) random copolymers (*c*-PNPG-*r*-PNBG) were prepared by NHC-mediated copolymerization of M_1 and *N*-butyl *N*-carboxyanhydride (M_2) with different initial $[M_1]_0$:$[M_2]_0$:$[NHC]_0$ ratios. The *c*-PNPG-*r*-PNBG copolymer composition and polymer M_n (Table 1, entry 7−12) were determined by ^{1}H NMR integration of the PNPG methylene protons (d) and the PNBG methine proton (g) relative to the phenyl proton (l) of the NHC moiety (Figure 5). Polymer M_ns and PDIs were also determined by SEC using a calibration curve constructed with monodisperse polystyrene standards (Table 1, entry 7−12). As the amount of M_2 incorporated into the *c*-PNPG-*r*-PNBG copolymer increases, the bimodal character of the SEC chromatogram appears to decrease, suggesting reduced aggregation of the *c*-PNPG-*r*-PNBG copolymers in the solution (Figure S12, Supporting Information).

Synthesis and Characterization of Cyclic and Linear Brush-Like Copolymers. Two azido-terminated poly(ethylene glycol) polymers (PEG-N_3) of different molecular weight (M_n = 2 kg·mol^{-1}, PDI = 1.03; M_n = 500 g·mol^{-1}, PDI = 1.05) were prepared by a previously reported procedure and their M_ns were determined by MALDI TOF MS analysis.[33] Grafting of PEG-N_3 to PNPG and $PNPG_n$-*ran*-$PNBG_m$ proceeded at room temperature in CH_2Cl_2 in the presence of CuBr/PMDETA (1:1) (~20−30 mol % relative to propargyl content) over a period of 3 h under nitrogen atmosphere (Scheme 3). The polymer product was purified by passing it through a neutral alumina column and precipitated by excess hexane.

Successful grafting of the polymeric side chains by CuAAC chemistry is evidenced by the appearance of characteristic triazolium protons at 8.0 ppm in the ^{1}H NMR spectrum of the polymer product (*c*-PNPG-*g*-PEG) (*k*, Figure S13, Supporting Information). The SEC analysis of the polymer product

Table 2. Cyclic Brush-Like Polymers with Poly(*N*-substituted glycine) Backbone and PEG Side Chains

entry	backbone composition[a]	backbone M_n[b] (kg·mol^{-1})	PEG M_n (g·mol^{-1})	$[N_3]_0$: $[propargyl]_0$	M_n[b] (kg·mol^{-1})	PDI[b]	Y_g[c] (%)	Y_g[d] (%)
1	*c*-$PNPG_{141}$	43.8	2k	0.5:1	121	1.68	19	-
2	*c*-$PNPG_{141}$	43.8	2k	0.8:1	174	2.28	19	-
3	*c*-$PNPG_{221}$-*r*-$PNBG_{196}$	44.6	2k	1.2:1	194	1.27	37	42
4	*c*-$PNPG_{221}$-*r*-$PNBG_{196}$	44.6	2k	1.5:1	204	1.23	47	45
5	*c*-$PNPG_{166}$-*r*-$PNBG_{33}$	49.2	550	0.75:1	142	1.82	45	-
6	*c*-$PNPG_{166}$-*r*-$PNBG_{33}$	49.2	550	2:1	175	1.73	62	-
7	*c*-$PNPG_{166}$-*r*-$PNBG_{33}$	49.2	550	3:1	145	1.78	77	-
8	*c*-$PNPG_{150}$-*r*-$PNBG_{30}$	49.2	550	1.6:1	155	1.71	52	-

[a] All reactions were carried out in THF (entries 1 and 2) or CH_2Cl_2 (entries 3−8) and the polymer composition is determined by ^{1}H NMR analysis. [b] All M_ns and PDIs were determined by SEC [LiBr(0.1M)/DMF, 50 °C] using polystyrene standards. [c] Grafting density was determined by ^{1}H NMR analysis. [d] Grafting density was determined by the changes of PEG-N_3 concentration, i.e., percentage intensity change of their SEC−DRI response.[11]

dx.doi.org/10.1021/ma201948u |*Macromolecules* 2011, 44, 9063–9074

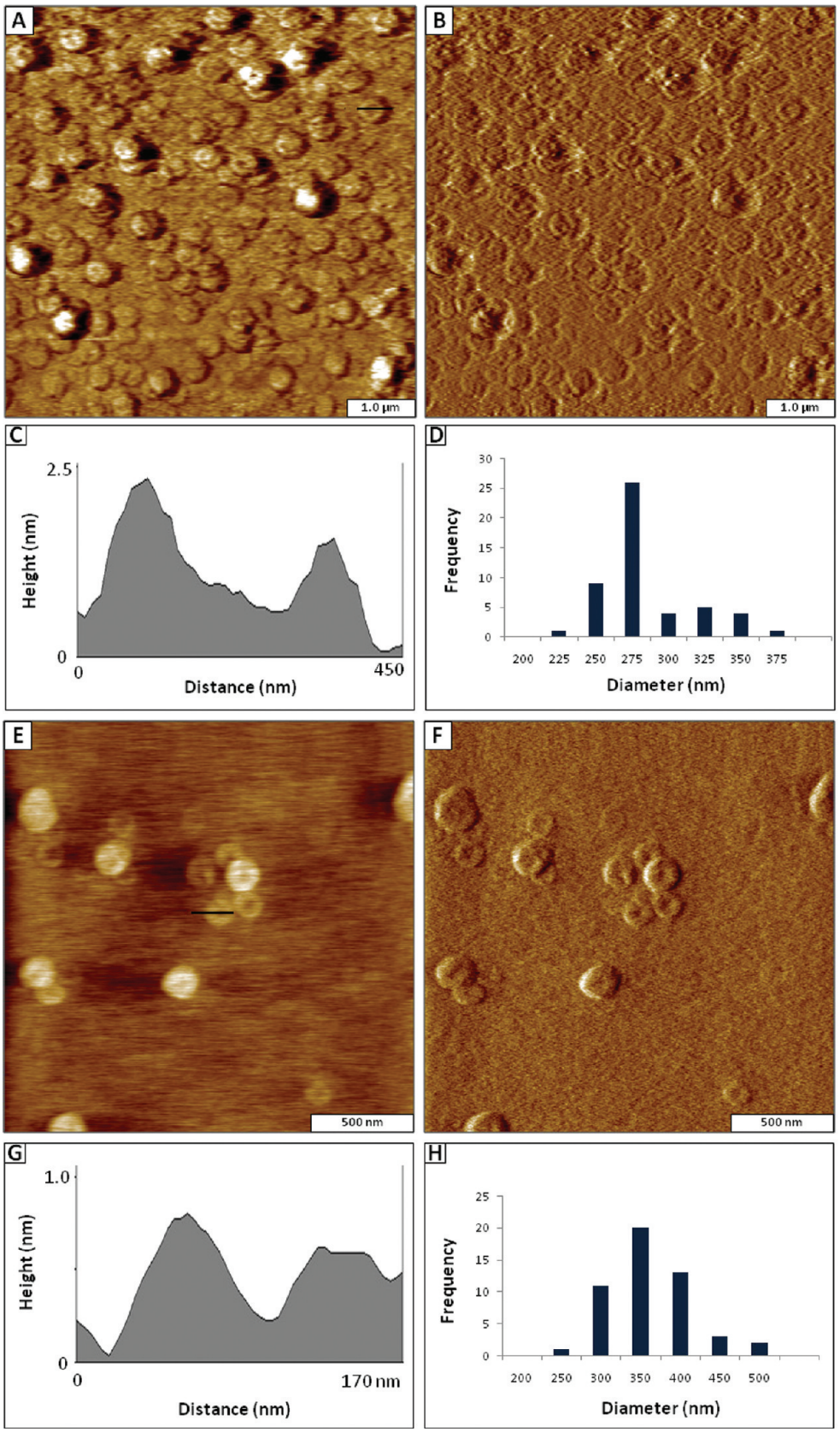

Figure 7. Representative AFM topographic (A, E) and amplitude (B, F) images of *c*-PNPG$_{141}$-*g*-(PEG2k)$_{27}$ and (*c*-PNPG$_{166}$-*r*-PNBG$_{33}$)-*g*-(PEG550)$_{154}$ (entry 1 and 7, Table 2) respectively on mica (0001) and the cross-section (C, G) and histogram analysis (D, H) of selected ring polymers within the respective sample (sampling size =50). (Note: the black line in Figure A and E indicate the specific nanostructure whose cross-section analysis is shown in Figure C and G.)

also reveals an increase in the molecular weight relative to that of *c*-PNPG, confirming successful grafting of the PEG side chains to the *c*-PNPG backbone (Figure 6). However, the molecular weight distribution is fairly broad (PDI = 1.68−2.28) (entry 1−2, Table 2). The integration ratio of the triazolium proton (*k*, Figure S13, Supporting Information) relative to the propargyl methine proton (*y*, Figure S13, Supporting Information) has been used to determine the grafting density ($Y_{GRAFTING}$). The maximum grafting density is ∼20%, which is low relative to typical polymer brushes prepared by the graft-to method (entry 1−2, Table 2).[11,36] Varying the ratio of $[N_3]_0$:$[propargyl]_0$ does not appear to have an appreciable effect in the grafting density. While steric crowding of the affixed polymeric side chains limits the grafting density, PNPG aggregation also contributes to the restricted access of propargyl groups by azido-ended PEG. As a result, we reason that random copolymers (*c*-PNPG-*r*-PNBG) will likely provide improved grafting efficiency due to the reduced aggregation tendency of these copolymers.

The side chain grafting density is indeed substantially increased to 37−77% (entry 3−8, Table 2), corresponding to high CuAAC coupling efficiency (70−93%), when the random copolymers (*c*-PNPG-*r*-PNBG) are used. The molecular weight distributions are also narrower (PDI = 1.23−1.82) than those obtained when *c*-PNPGs are used in the PEG grafting experiments. The grafting density was determined by integrating the resonance for the single triazolium proton (*k*, Figure S14, Supporting Information) relative to the three protons on the methyl group of the PNBG repeating unit (*i*, Figure S14, Supporting Information), which is then multiplied by the molar percentage of PNBG repeating unit in the random copolymers. Grafting densities can also be enhanced by increasing the ratio of $[N_3]_0$:$[propargyl]_0$ (entries 5−7, Table 2). We have shown that increasing PNBG content results in reduced aggregation of the random copolymers *c*-PNPG-*r*-PNBG, as manifested in increasingly monomodal SEC chromatograms (Figure S12, Supporting Information). The molecular weight distribution (PDI) of the cyclic brush-like polymers [i.e., (*c*-PNPG-*r*-PNBG)-*g*-PEG] also appears to decrease with increasing PNBG backbone content, suggesting that perhaps the reduced aggregation facilitates the statistical grafting of the side chains, resulting in lowered PDIs (entry 3−8, Table 2).

To further validate the grafting density obtained by ^{1}H NMR analysis, we quantified the percentage decrease of PEG-N_3 content prior to and post CuAAC by the SEC-DRI method (Figure S15, Supporting Information).[11] As the initial $[N_3]_0$:$[propargy]_0$ ratio is known, the grafting density can be deduced. The grafting densities obtained by ^{1}H NMR or SEC analysis are in good agreement (entry 3−4, Table 2). Linear brush-like copolymers [(*l*-PNPG-*r*-PNBG)-*g*-PEG] can also be synthesized in a similar manner as the cyclic analogs with high grafting efficiency.

AFM Analysis of Cyclic Brush-Like Copolymers. Atomic force microscopic (AFM) analysis of the cyclic brush-like polymers [i.e., *c*-$PNPG_{141}$-*g*-$(PEG2k)_{27}$ and (*c*-$PNPG_{166}$-*r*-$PNBG_{33}$)-*g*-$(PEG550)_{154}$] (entry 1 and 7, Table 2) is presented in Figure 7. Bright areas in the topography images (Figure 7, parts A and E) display disc- or ring-shaped nanostructures, which exhibit a narrow size distribution. The darker areas in these topographical figures are considered to be the mica background. The height profiles for all samples were relatively low (<2.5 nm), consistent with a single layer of nanostructures lying flat on the mica surface (Figure 7, parts C and G). Amplitude images constructed by mapping the cantilever oscillation as it is raster scanned across the surface also reveal ring-shaped nanostructures (Figure 7, parts B and F). Differences in the nanostructure size were observed for the cyclic brush-like polymers with variable composition. The cross-section and histogram analysis of the nanostructures reveals an average diameter of 283 and 362 nm for *c*-$PNPG_{141}$-*g*-$(PEG2k)_{27}$ and (*c*-$PNPG_{166}$-*r*-$PNBG_{33}$)-*g*-$(PEG550)_{154}$ respectively (Figure 7, parts D and H). The lateral dimensions are exaggerated when compared to the theoretical diameters based on the polymer composition (i.e., 49 and 32 nm). This is attributed to the tip effect in AFM imaging that displays a convolution of the geometry of the sample and tip, resulting in overestimation of the lateral features.[37]

While the 'donut-shape' is not as evident for *c*-$PNPG_{141}$-*g*-$(PEG2k)_{27}$ (Figure 7, parts A and B), it is clearly visible for (*c*-$PNPG_{166}$-*r*-$PNBG_{33}$)-*g*-$(PEG550)_{154}$ (Figures 7, parts E and F). This is likely to arise from the difference in side chain length relative to the diameter of the cyclic backbone. If the cyclic backbone and the side chains are assumed to adopt a fully extended zigzag conformation, the cyclic backbone diameter of *c*-$PNPG_{141}$-*g*-$(PEG2k)_{27}$ is estimated to be 17 nm and PEG chain length is 16 nm, resulting in a theoretical diameter of 49 nm for the nanostructure. In comparison, the theoretical diameter of the (*c*-$PNPG_{166}$-*r*-$PNBG_{33}$)-*g*-$(PEG550)_{154}$ nanostructure is estimated to be 32 nm, which is the sum of the cyclic backbone diameter (24 nm) and the twice the PEG side chain length (4 nm). As a result, one would expect to observe a "donut hole" in the AFM images of the latter sample, but not necessarily the former. Additionally, the cyclic brush-like polymers can also self-assemble into larger aggregates (Figure S16, Supporting Information), but small ring nanostructures are still visible along with the aggregates. By contrast, AFM imaging of the linear brush-like polymer (*l*-PNPG-*r*-PNBG)-*g*-PEG reveals only large and ill-defined aggregates.

CONCLUSIONS

The monomer *N*-propargyl *N*-carboxyanhydrides were successfully polymerized using NHC initiators to yield cyclic poly(*N*-propargyl glycine) (*c*-PPNG) in a controlled manner. The propargyl groups enable further side chain derivation by CuAAC chemistry. This was demonstrated in the synthesis of brush-like polymers having poly(*N*-substituted glycine) backbone and PEG side chain. The grafting efficiency of polymer side chain is low when *c*-PPNG homopolymer is used, presumably due to polymer aggregation that hinders access to the propargyl groups. High-to-quantitative grafting efficiencies can be obtained by utilizing cyclic random block copolymers (i.e., PPNG-*r*-PBNG) where the reactive propargyl groups are spaced by inert butyl side chains. The increase in grafting density is attributed to either a decrease in cyclic backbone aggregation in the CuAAC reaction medium or a decrease in steric crowding among the side chains on the cyclic backbones. The AFM analysis of the cyclic brush-like polymers reveals the formation of donut-shape nanostructures whose dimension correlates well with the molecular composition of the polymers. The successful development of NHC-mediated polymerization of NCA bearing side chains amendable to CuAAC chemistry will enable future development of structurally and functionally diverse polymer materials with novel architectures. For example, appending thermo- and pH-responsive side chains on to the cyclic backbones will produce stimuli-responsive

nano-objects useful for drug delivery applications or smart membranes. Cyclic brush-like polymers bearing mutually incompatible side chains are potentially useful as polymeric blend compatibilizers.

■ ASSOCIATED CONTENT

Supporting Information. Time-dependent FTIR spectra of a NHC-mediated polymerization of M_1, ^{1}H NMR, ESI MS, MALDI−TOF MS spectra of the polymer product from NHC-mediated polymerizations of M_1 prior to removal of cyclic oligomers, the molar percentage of M_1, *c*-PNPG, and 6MR as a function of polymerization time, the plot of the observed rate constant (k_{obs}) versus the initial NHC concentration, SEC chromatograms of *c*-PNPG, *l*-PNPG, and *c*-PNPG-*r*-PNBG, DLS traces of *c*-PNPG in THF, ^{1}H NMR spectrum of *l*-PNPG, the polymerization results of $BuNH_2$-initiated polymerizations of M_1 to yield *l*-PNPG, Mark−Houwink−Sakurada plot for *c*-PNPG and *l*-PNPG, ^{1}H NMR spectra of *c*-PNPG-*g*-PEG and *c*-PNPG-*r*-PNBG-*g*-PEG, SEC chromatograms that display the conversion of *c*-PNPG-*r*-PNBG into *c*-PNPG-*r*-PNBG-*g*-PEG, and AFM images of *c*-PNPG-*r*-PNBG-*g*-PEG (entry 8, Table 2) along with the section and histogram analysis. This material is available free of charge via the Internet at http://pubs.acs.org.

■ AUTHOR INFORMATION

Corresponding Author
*E-mail: dhzhang@lsu.edu.

■ ACKNOWLEDGMENT

The authors thank Dr. Rafael Cueto for assisting with the SEC studies. S.H.L. thanks Dr. Haoyu Tang for helpful discussion. This work was supported by Louisiana State University, the National Science Foundation (CHE-0955820 and DMR-0906873), and Louisiana State Board of Regents [LEQSF(2008-11)-RD-A-11]. W.K.S. acknowledges financial support for study-leave from Masinde Muliro University in Kenya.

■ REFERENCES

(1) Muir, H. *Biochem. Soc. Trans.* **1983**, *11*, 613–622.
(2) Wintermantel, M.; Gerle, M.; Fischer, K.; Schmidt, M.; Wataoka, I.; Urakawa, H.; Kajiwara, K.; Tsukahara, Y. *Macromolecules* **1996**, *29*, 978–983.
(3) Zhang, M.; Müller, A. H. E. *J. Polym. Sci., Part A: Polym. Chem.* **2005**, *43*, 3461–3481.
(4) Sheiko, S. S.; Sun, F. C.; Randall, A.; Shirvanyants, D.; Rubinstein, M.; Lee, H.-i.; Matyjaszewski, K. *Nature* **2006**, *440*, 191–194.
(5) Huang, K.; Rzayev, J. *J. Am. Chem. Soc.* **2009**, *131*, 6880–6885.
(6) Müller, M. T.; Yan, X.; Lee, S.; Perry, S. S.; Spencer, N. D. *Macromolecules* **2005**, *38*, 5706–5713.
(7) Kumaraswamy, G.; Dibaj, A. M.; Caruso, F. *Langmuir* **2002**, *18*, 4150–4154.
(8) Sheiko, S. S.; Sumerlin, B. S.; Matyjaszewski, K. *Prog. Polym. Sci.* **2008**, *33*, 759–785.
(9) Yamada, K.; Miyazaki, M.; Ohno, K.; Fukuda, T.; Minoda, M. *Macromolecules* **1998**, *32*, 290–293.
(10) Beers, K. L.; Gaynor, S. G.; Matyjaszewski, K.; Sheiko, S. S.; Moller, M. *Macromolecules* **1998**, *31*, 9413–9415.
(11) Gao, H.; Matyjaszewski, K. *J. Am. Chem. Soc.* **2007**, *129*, 6633–6639.
(12) Binder, W. H.; Sachsenhofer, R. *Macromol. Rapid Commun.* **2008**, *29*, 952–981.
(13) Kolb, H. C.; Sharpless, K. B.; Finn, M. G. *Angew. Chem., Int. Ed.* **2001**, *40*, 2004–2021.
(14) (a) Sumerlin, B. S.; Tsarevsky, N. V.; Louche, G.; Lee, R. Y.; Matyjaszewski, K. *Macromolecules* **2005**, *38*, 7540–7545. (b) Helms, B.; Mynar, J. L.; Hawker, C. J.; Fréchet, J. M. J. *J. Am. Chem. Soc.* **2004**, *126*, 15020–15021. (c) Parrish, B.; Breitenkamp, R. B.; Emrick, T. *J. Am. Chem. Soc.* **2005**, *127*, 7404–7410.
(15) (a) Gondi, S. R.; Vogt, A. P.; Sumerlin, B. S. *Macromolecules* **2007**, *40*, 474–481. (b) Golas, P. L.; Matyjaszewski, K. *Chem. Soc. Rev.* **2010**, *39*, 1338–1354. (c) Meldal, M. *Macromol. Rapid Commun.* **2008**, *29*, 1016–1051. (d) Tsarevsky, N. V. *J. Polym. Sci., Part A: Polym. Chem.* **2010**, *48*, 966–974. (e) Wu, J.; Gao, C. *Macromolecules* **2010**, *43*, 7139–7146. (f) Zhang, Y.; He, H.; Gao, C. *Macromolecules* **2008**, *41*, 9581–9594. (g) Li, C.; Ge, Z.; Fang, J.; Liu, S. *Macromolecules* **2009**, *42*, 2916–2924. (h) Fu, G. D.; Xu, L. Q.; Yao, F.; Zhang, K.; Wang, X. F.; Zhu, M. F.; Nie, S. Z. *ACS Appl. Mater. Interfaces* **2009**, *1*, 239–243. (i) Yuan, Y.-Y.; Du, Q.; Wang, Y.-C.; Wang, J. *Macromolecules* **2010**, *43*, 1739–1746.
(16) Kreutzer, G.; Ternat, C.; Nguyen, T. Q.; Plummer, C. J. G.; Månson, J.-A. E.; Castelletto, V.; Hamley, I. W.; Sun, F.; Sheiko, S. S.; Herrmann, A.; Ouali, L.; Sommer, H.; Fieber, W.; Velazco, M. I.; Klok, H.-A. *Macromolecules* **2006**, *39*, 4507–4516.
(17) Schappacher, M.; Deffieux, A. *Science* **2008**, *319*, 1512–1515.
(18) (a) Schappacher, M.; Deffieux, A. *J. Am. Chem. Soc.* **2008**, *130*, 14684–14689. (b) Schappacher, M.; Deffieux, A. *Angew. Chem., Int. Ed.* **2009**, *48*, 5930–5933.
(19) Jia, Z.; Fu, Q.; Huang, J. *Macromolecules* **2006**, *39*, 5190–5193.
(20) Coulembier, O.; Moins, S. b.; De Winter, J.; Gerbaux, P.; Leclére, P.; Lazzaroni, R.; Dubois, P. *Macromolecules* **2010**, *43*, 575–579.
(21) (a) Xia, Y.; Boydston, A. J.; Grubbs, R. H. *Angew. Chem., Int. Ed.* **2011**, *50*, 5882–5885. (b) Zhang, K.; Lackey, M. A.; Wu, Y.; Tew, G. N. *J. Am. Chem. Soc.* **2011**, *133*, 6906–6909.
(22) (a) Semlyen, J. A. *Cyclic Polymers*; Kluwer Academic Publishers: Norwell, MA, 2000. (b) Laurent, B. A.; Grayson, S. M. *Chem. Soc. Rev.* **2009**, *38*, 2202–2213.(c) Kobayashi, S.; Endo, K. In *New Frontiers in Polymer Synthesis*; Springer: Berlin and Heidelberg, Germany, 2008, 217, 121−183. (d) Kricheldorf, H. R. *J. Polym. Sci., Part A: Polym. Chem.* **2010**, *48*, 251–281.
(23) (a) Laurent, B. A.; Grayson, S. M. *J. Am. Chem. Soc.* **2006**, *128*, 4238–4239. (b) Whittaker, M. R.; Goh, Y.-K.; Gemici, H.; Legge, T. M.; Perrier, S.; Monteiro, M. J. *Macromolecules* **2006**, *39*, 9028–9034. (c) Misaka, H.; Kakuchi, R.; Zhang, C.; Sakai, R.; Satoh, T.; Kakuchi, T. *Macromolecules* **2009**, *42*, 5091–5096.
(24) Stanford, M. J.; Pflughaupt, R. L.; Dove, A. P. *Macromolecules* **2010**, *43*, 6538–6541.
(25) (a) Schappacher, M.; Deffieux, A. *J. Am. Chem. Soc.* **2011**, *133*, 1630–1633. (b) Schappacher, M.; Deffieux, A. *Macromolecules* **2011**, *44*, 4503–4510. (c) Hu, J.; Zheng, R.; Wang, J.; Hong, L.; Liu, G. *Macromolecules* **2009**, *42*, 4638–4645.
(26) Szymanski, R.; Kubisa, P.; Penczek, S. *Macromolecules* **1983**, *16*, 1000–1008.
(27) Jacobson, H.; Beckmann, C. O.; Stockmayer, W. H. *J. Chem. Phys.* **1950**, *18*, 1607–1612.
(28) Kricheldorf, H. R.; Schwarz, G. *Macromol. Rapid Commun.* **2003**, *24*, 359–381.
(29) (a) Bielawski, C. W.; Benitez, D.; Grubbs, R. H. *Science* **2002**, *297*, 2041–2044. (b) Li, H.; Debuigne, A.; Jérome, R.; Lecomte, P. *Angew. Chem., Int. Ed.* **2006**, *45*, 2264–2267. (c) Herbert, D. E.; Gilroy, J. B.; Chan, W. Y.; Chabanne, L.; Staubitz, A.; Lough, A. J.; Manners, I. *J. Am. Chem. Soc.* **2009**, *131*, 14958–14968. (d) Culkin, D. A.; Jeong, W.; Csihony, S.; Gomez, E. D.; Balsara, N. P.; Hedrick, J. L.; Waymouth, R. M. *Angew. Chem., Int. Ed.* **2007**, *46*, 2627–2630. (e) Jeong, W.; Hedrick, J. L.; Waymouth, R. M. *J. Am. Chem. Soc.* **2007**, *129*, 8414–8415. (f) Jeong, W.; Shin, E. J.; Culkin, D. A.; Hedrick, J. L.; Waymouth, R. M. *J. Am. Chem. Soc.* **2009**, *131*, 4884–4891. (g) Shin, E. J.; Brown, H. A.; Gonzalez, S.; Jeong, W.; Hedrick, J. L.; Waymouth, R. M. *Angew. Chem., Int. Ed.* **2011**, *50*, 6388–6391. (h) Guo, L.; Zhang, D. *J. Am. Chem. Soc.* **2009**, *131*, 18072–18074. (i) Guo, L.; Li, J.; Brown, Z.; Ghale, K.; Zhang, D. *Biopolym.: Peptide Sci.* **2011**, *96*, 596–603.

(30) Patch, J. A.; Barron, A. E. *Curr. Opin. Chem. Biol.* **2002**, *6*, 872–877.
(31) Barron, A. E.; Zuckermann, R. N. *Curr. Opin. Chem. Biol.* **1999**, *3*, 681–687.
(32) Arduengo, A. J.; Krafczyk, R.; Schmutzler, R.; Craig, H. A.; Goerlich, J. R.; Marshall, W. J.; Unverzagt, M. *Tetrahedron* **1999**, *55*, 14523–14534.
(33) Ostaci, R.-V.; Damiron, D.; Grohens, Y.; Léger, L.; Drockenmuller, E. *Langmuir* **2009**, *26*, 1304–1310.
(34) Li, X.; Guo, L.; Casiano-Maldonado, M.; Zhang, D.; Wesdemiotis, C. *Macromolecules* **2011**, *44*, 4555–4564.
(35) Beste, L. F.; Hall, H. K., Jr. *J. Phys. Chem.* **1964**, *68*, 269–274.
(36) (a) Ostaci, R.-V.; Damiron, D.; Capponi, S.; Vignaud, G.; Leger, L.; Grohens, Y.; Drockenmuller, E. *Langmuir* **2008**, *24*, 2732–2739. (b) Fallais, I.; Devaux, J.; Jérôme, R. *J. Polym. Sci., Part A: Polym. Chem.* **2000**, *38*, 1618–1629.
(37) Villarrubia, J. S. *J. Res. Natl. Inst. Stand. Technol.* **1997**, *102*, 425–454.